Measurements of the thermopower coefficient above the superconducting transition in polycrystalline $Y_1Ba_2Cu_3O_{7-\delta}$: absence of appreciable fluctuation effects

Measurements of the thermopower coefficient above the superconducting transition in polycrystalline $Y_1Ba_2Cu_3O_{7-\delta}$: absence of appreciable fluctuation effects

O Cabeza, A Pomar, A Díaz, C Torrón, J A Veira, J Maza and Félix Vidal

Laboratorio de Física de Materiales, Departamento de Física de la Materia Condensada, Universidad de Santiago de Compostela, 15706, Spain

Abstract. This paper reports on detailed measurements of the thermoelectric power coefficient, $L(T) \equiv S(T)\sigma(T)$, relating the thermoelectric power $S(T)$ to the electrical conductivity $\sigma(T)$ in three polycrystalline $Y_1Ba_2Cu_3O_{7-\delta}$ samples. All the samples have almost the same composition ($\delta \gtrsim 0.10$) and they are single-phase to within 4%, but they have very different structural inhomogeneities at long length scales, i.e. at scales much larger than the superconducting correlation length in all directions. Our measurements in different single-phase samples indicate that all the critical behaviour of $S(T)$ above the superconducting transition is driven by $\sigma(T)$. Therefore, these results strongly suggest, within our experimental resolutions of $\Delta L/L \gtrsim 2\%$, that $L(T)$ in $Y_1Ba_2Cu_3O_{7-\delta}$ compounds is not affected, over the entire mean-field-like region (MFR) above the superconducting transition, by thermodynamic fluctuations of the superconducting order parameter amplitude (OPF). The reduced temperature behaviour of the thermopower excess $\Delta S(\epsilon)$ is the same for all the single-phase samples studied here, i.e. fractal effects are not observed in the MFR, in agreement with our previous paraconductivity results. Also, the OPF effects arising on $S(T)$ through $\sigma(T)$ are confirmed to be essentially three-dimensional (3D) over the entire MFR.

1. Introduction

Until the discovery of high-temperature copper oxide superconductors (HTSC), the influence of the thermodynamic fluctuations of the superconducting order parameter amplitude (OPF) on the thermoelectric power S in superconductors remained as an interesting but mainly academic problem [1,2]. These effects could not be observed in bulk low-temperature metallic superconductors (LTS). This was mainly due to the fact that their superconducting order parameter correlation length amplitude $\xi(0)$ was relatively important, typically of the order of 1000 Å. As a consequence, the temperature range over which one might expect to see OPF effects would be very small (see e.g. [1–3]), orders of magnitude less than the temperature differences needed to measure S. In the copper oxide superconductors, however, $\xi(0)$ is typically two orders of magnitude smaller than in LTS (so, the coherent volume in bulk samples is six orders of magnitude smaller) and, therefore, OPF effects will manifest themselves at easily accessible temperature differences from the superconducting transition. For instance, measurements of the electrical resistivity $\rho(T)$ or of the magnetic susceptibility

$\chi(T)$ indicate that in HTSC the OPF effects are appreciable even 10 K above the superconducting transition [4–7].

In spite of their interest and of the experimental advantages indicated above, the OPF effects on $S(T)$ above the superconducting transition in HTSC have been relatively little studied until now, and the emerging picture is rather confusing. For instance, in the case of single-crystal and polycrystal $Y_1Ba_2Cu_3O_{7-\delta}$ and related samples, most of the measurements indicate a relatively rounded peak of $S(T)$ above the transition [8–14], although in some studies a very sharp peak of $S(T)$ has been observed just above the transition [15, 16]. Some authors have claimed that such a sharp peak is due to OPF effects [16], although it could just be a spurious effect associated with sample temperature inhomogeneities (see e.g. [14]). The discrepancies concerning the OPF effects remain even among those papers that propose a qualitatively similar rounded $S(T)$ peak above the transition. For instance, some authors propose that the OPF effects, alone [11] or combined with other mechanisms (see e.g. [17]), causes the $S(T)$ rounded peak itself. However, first Laurent and coworkers [9, 10, 18] and then Cabeza and coworkers [12, 13, 19], taking into account that the measured $S(T)$ depends strongly on the electrical resistivity, have proposed that the OPF effects probably cause the rounding of the $S(T)$ peak above the transition, but not at all the peak itself, which will be associated with transport effects in the normal phase [20–26]. But important discrepancies still remain between the proposals of these last authors in what concerns basic aspects of the OPF effects on $S(T)$. For instance, Laurent and coworkers have proposed two- (2D) and four- (4D) dimensional OPF in $Y_1Ba_2Cu_3O_{7-\delta}$ compounds [9, 10], and fractal dimensionality in Bi-based materials [10, 18]. These proposals are not only in contrast with our results on $S(T)$ rounding [12, 13, 19], but also with extensive work made in HTSC on the electrical resistivity [4, 5] and on the magnetic susceptibility [6, 7] roundings above the transition, which clearly support the 3D and 2D nature of OPF in the mean-field region (MFR), i.e. from approximately 1 K to 10 K from the transition for, respectively, Y-based and Bi-based superconductors.

In fact, such a basic and old question as the possible influence of OPF effects on the thermopower coefficient $L(T)$, relating $S(T)$ to the electrical conductivity $\sigma(T)$ by

$$L(T) \equiv S(T)\sigma(T) \tag{1}$$

still remains to be answered at a quantitative level. Is $L(T)$ in HTSC appreciably affected by OPF effects in the mean-field-like region (MFR)? In this paper we will try to answer this question quantitatively. For that purpose, we present simultaneous measurements of the $S(T)$ and of the $\rho(T)$ roundings above the superconducting transition in three single-phase (to within 4%) $Y_1Ba_2Cu_3O_{7-\delta}$ polycrystalline samples, all with the same nominal composition and with $\delta \lesssim 0.10$, but having very distinct long length scale structural inhomogeneities. For the first time, an empirical picture is proposed to account for the influence on $S(T)$ of these structural inhomogeneities. The OPF effects on both quantities, extracted following consistent procedures, will be compared with one another and with the existing theories. Also, for the first time, our results confirm to a quantitative level our previous qualitative proposal [12] that the thermopower coefficient $L(T)$, relating $S(T)$ to $\sigma(T)$, is not affected in $Y_1Ba_2Cu_3O_{7-\delta}$ compounds by the presence of OPF. This finding seems to be confirmed by a recent theoretical calculation of $\Delta L(\epsilon)$ in the MFR in layered superconductors [27].

2. Experimental details

Three batches of granular $Y_1Ba_2Cu_3O_{7-\delta}$ ceramic (YBCO) samples with $\delta \lesssim 0.10$ were used. All the samples were prepared by the usual solid-state synthesis procedure [28]. For the first batch of samples (denoted Y1), constituent oxides, mixed in stoichiometric ratio, were heated at 950 °C for 24 h. The product was powdered, pelletized and sintered at 900 °C for 6 h in an oxygen atmosphere and then cooled to 200 °C without cutting the oxygen flow. Material was maintained at this temperature for 2 h. For the second batch of samples (Y2), the constituent oxides, mixed in stoichiometric ratio, were finally treated in air at 400 °C for 7 days, followed by quenching in liquid nitrogen. The third batch of samples (Y3) was prepared in the same way, except that the final product was slowly cooled down in an air atmosphere.

All the samples are single-phase within 4%, as shown by x-ray analysis. Optical microscopy measurements and scanning electron microscopy (SEM) show that the typical grain and crystallite size of our polycrystalline samples are 1 to 30 μm. The crystallites also show a high density of twin boundaries at a length scale larger than 1000 Å. The main structural difference between the various samples concerns the pores among the grains. In some of the samples these pores are relatively important, and they have the same length scales as the grains and crystallites. This porosity reduces the sample average density to 80% of the ideal one, and also contributes to increasing the normal resistivity by one or two orders of magnitude over that of single crystals, ρ_{ab}. The average density of the less porous samples is of the order of 90% of the ideal one, and $\rho(T)$ in the normal state is only few times bigger than $\rho_{ab}(T)$. In contrast with these important resistivity differences, the amplitude of $S(T)$ for the various samples is always of the same order of magnitude as $S_{ab}(T)$ in single crystals (see later).

We first recall that the absolute thermoelectric power S may be easily defined through J_N, the number current density [29]

$$- J_N = (\sigma/e^2)\nabla\mu + (\sigma S/e)\nabla T \tag{2}$$

where e is the carrier's electric charge, σ is the electrical conductivity, ∇T is the temperature gradient, and

$$\mu = \mu_c + \mu_e \tag{3}$$

where μ_c is the chemical potential and $\mu_e = -eV_e$, with V_e being the ordinary electrostatic potential. To measure S, we employ the standard DC differential method under the condition $J_N = 0$, which yields [30]

$$\frac{\Delta V}{\Delta T} = -\frac{1}{\Delta T}\int_{T-\Delta T/2}^{T+\Delta T/2} S(T')\,dT' + \frac{1}{\Delta T}\int_{T-\Delta T/2}^{T+\Delta T/2} S_{\text{leads}}(T')\,dT' \tag{4}$$

where ΔT and T are, respectively, the difference and the mean of both sample end temperatures, and ΔV is the potential difference between leads (hot branch minus cold branch) measured at the voltmeter terminals. Since S_{leads} (in our case copper) is non-singular at liquid N_2 temperatures and above, one can approximate for moderate temperature differences,

$$S_M(T) \equiv \frac{1}{\Delta T}\int_{T-\Delta T/2}^{T+\Delta T/2} S(T')\,dT' \simeq S_{\text{leads}}(T) - \frac{\Delta V}{\Delta T} \tag{5}$$

from which one can obtain the measured (average) thermopower S_M, once S_{leads} is known. Note that $\Delta V/\Delta T$ and, therefore, $S_M(T)$ do not depend on the sample geometrical parameters. In other words, the determination of the absolute thermopower does not need detailed knowledge of the sample geometry, in contrast with, for instance, the experimental determination of the sample electrical resistivity. We will see in section 3 that this is an important advantage in the case of polycrystalline samples, where some undetermined porosity may be present.

The unavoidable use of a small but finite temperature gradient to obtain the intrinsic thermopower $S(T)$ is irrelevant when $S(T)$ has a mild temperature dependence. However, such a temperature gradient may introduce spurious differences between $S_M(T)$ and $S(T)$ near the superconducting transition [9]. To obtain $S(T)$ from $S_M(T)$, i.e. to eliminate the spurious effects generated near the transition by the finite temperature gradient, we have used a numerical procedure. Essentially, this procedure consists of inverting equation (5) and recasting it into the form:

$$S(T - n\Delta T) = S(T) - \Delta T \sum_{m=0}^{n-1} \frac{dS_M}{dT}\left(T - \frac{\Delta T}{2} - m\Delta T\right) \qquad (6)$$

where m and n are integers. This expression relates $S(T)$ to $S(T - n\Delta T)$ through the derivatives of the measured thermopower. Its application entails the following steps. First, we take T to be a fixed temperature well above the superconducting transition (say 110 K in our case) where one can neglect the non-zero temperature gradient effects on $S(T)$, i.e. where one can assume $S(T) \simeq S_M(T)$. Then, the evaluation of the derivatives dS_M/dT at the discrete temperatures $T-(\Delta T/2)-m\Delta T$ $(m = 1, 2, \ldots, n-1)$ yields directly $S(T-n\Delta T)$. Reconstruction of $S(T)$ is accomplished by sweeping in n, so that $T - n\Delta T$ spans in temperature the entire transition. Note that this procedure (from $S_M(T)$ to $S(T)$) is just the reversed one (from $S(T)$ to $S_M(T)$) reported by Laurent and coworkers in order to single out the effects of the ΔT-induced spurious roundings [9].

The samples, with typical size $10 \times 2 \times 1$ mm^3, were mounted on a specially designed sample holder assembly made of copper. The schematic diagram of the low-temperature portion of the apparatus is shown in figure 1. As illustrated in this figure, the HTSC sample was fixed, symmetrically, between two microheaters with the help of a spring arrangement. The main microheater was fixed with an isolated PVC plate, whereas the auxiliary microheater was fixed at a copper block. The sample holder assembly was placed in a stainless-steel cavity, and the cavity was in contact with the cold tip of the cryostat. The microheaters were made by winding insulated constantan heater wire (diameter 0.1 mm) on small aluminium blocks, and they were capable of giving several milliwatts power. In order to avoid heat losses, due for instance to radiation, the microheaters were embedded in teflon. GE Varnish 7031 was applied at both ends of the sample for better thermal contact with the microheaters. The required temperature gradient across the sample was created by adjusting the current in the microheaters.

Two copper-constantan thermocouples (type T), calibrated with a RhFe thermometer, were used to monitor the temperature gradient across the sample. As average sample temperature, we use half of the sum of the temperatures measured by these two thermocouples. Two platinum resistance thermometers were also used to control the sample end temperatures. A pair of copper leads (diameter 0.1 mm),
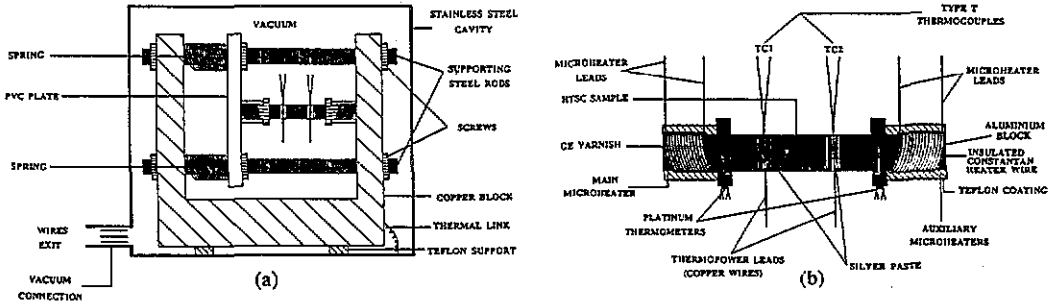
Figure 1. Schematic diagrams of the low-temperature portion of the experimental set-up used to measure $S(T)$ and $\rho(T)$: (a) general view; (b) detail of the sample mounted for measurement.

attached to the sample with a minute amount of silver paste (Dupont 4929), were used to record the thermal voltage. The temperature difference was kept to within 0.5 to 1 K cm^{-1} and we have checked that $\Delta V/\Delta T$ is constant over that temperature gradient range. The temperature sweeping rate was about 5 K h^{-1}. An automated data acquisition system comprising an $8\frac{1}{2}$ digit voltmeter with scanner and controller was used for data acquisition. Electrical resistivity of the samples was measured with a four-probe technique using the same data acquisition system as for S. Electrical resistivity and thermoelectric power resolutions were, respectively, 1 $\mu\Omega$ cm and 0.1 μV K^{-1}. Temperature resolution was 10 mK for $\rho(T)$ and 50 mK for $S(T)$. Lastly, measured S data were corrected for the copper leads contribution, S_{leads} in equation (5), according to standard tables [30].
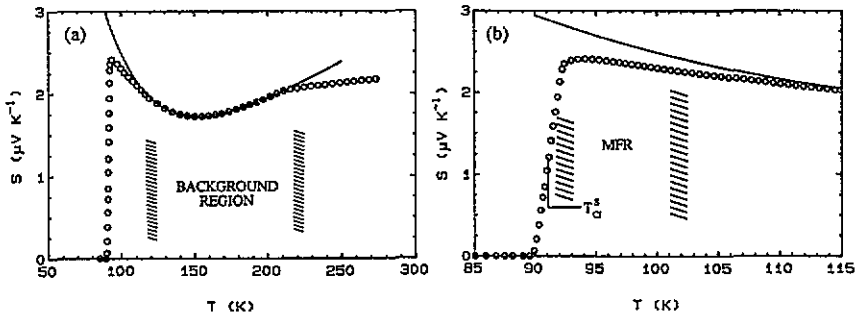

Figure 2. Temperature behaviour of the measured thermoelectric power of sample Y2. The full curve represents the $S(T)$ background. (a) Over all the temperature region measured, showing the background region. (b) Near the transition, showing the temperature where $S(T)$ has its inflection point (T_{ci}^S) and the mean-field-like region (MFR).

3. Experimental results

As an example of our $S(T)$ results, in figures 2(a) and (b) we represent the temperature dependence of the thermoelectric power for sample Y2, in the zero

temperature gradient limit. The full curves in (a) and (b) are the thermopower background $S_B(T)$, and they correspond to the expression [31]

$$S_B(T) = aT[1 + b\exp(-T/T_0)] \tag{7}$$

where a, b and T_0 are free parameters. We do not claim this functional form to represent better than others the physics of thermopower in the normal state, but as indicated before for $\rho_B(T)$ [4, 5, 32], equation (7) gives a high-quality fitting over a wide T region well above the transition, in the so-called background region, i.e. in the normal region where the OPF effects become negligible.
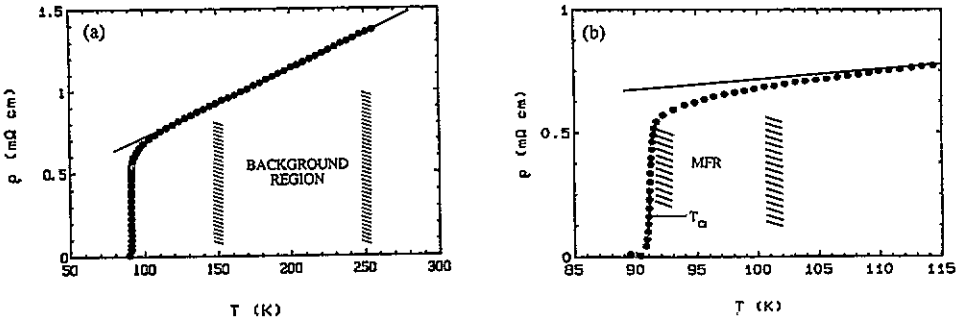

Figure 3. Temperature behaviour of the measured electrical resistivity of sample Y2. The full line represents the $\rho(T)$ background. (a) Over all the temperature region measured, showing the background region. (b) Near the transition, showing the temperature where $\rho(T)$ has its inflection point (T_{CI}) and the mean-field-like region (MFR).

In figures 3(a) and (b) we represent the temperature dependence of the measured electrical resistivity of the same sample as in figure 2. From these $\rho(T)$ data we may extract $\rho_{ab}(T)$, the intrinsic resistivity in the ab plane of an ideal single-crystal sample with the same nominal composition as the Y2 sample. For that we use the empirical relationship between $\rho(T)$ and $\rho_{ab}(T)$ proposed before [4–7, 32]

$$\rho(T) = (1/p)[\rho_{ab}(T) + \rho_{ct}]. \tag{8}$$

This equation is supposed to be valid above T_{CI} (the temperature where $\rho(T)$ around the transition has its inflection point). In equation (8), the coefficients p and ρ_{ct} are associated with the structural inhomogeneities at long length scales, i.e. at length scales much larger than the superconducting correlation length in all directions; p ($0 \leqslant p \leqslant 1$) is associated with the effective cross section of the sample and with the path lengthening due to the random orientation of the ab planes of the different sample domains (grains, untwinned regions, etc), and ρ_{ct} accounts for the average contact resistance between different sample domains. Above T_{CI}, p and ρ_{ct} are supposed to be constant, and they are extracted for each sample by comparing its normal resistivity far away from the transition (150 K $\leqslant T \leqslant$ 250 K, to avoid the presence of critical phenomena [4, 5]) with the resistivity in the ab plane of a single crystal of the same composition ($p \simeq 1$, $\rho_{ct} \simeq 0$). The available $\rho_{ab}(T)$ in different single crystals are well fitted, in this background region by [33]

$$\rho_{abB}(T) = C_1 + C_2 T \tag{9}$$

with $C_1 = 5 \pm 15 \ \mu\Omega$ cm and $C_2 = 0.5 \pm 0.2 \ \mu\Omega$ cm K^{-1}, which corresponds to the average values from the data of [33]. The full line in figure 3(a) is the measured resistivity background obtained by extrapolating through the transition the resistivity measured in the background region (150 K $\leqslant T \leqslant$ 250 K). Note that a practicable way to characterize the sample structural inhomogeneities at long length scales is through the p value in equation (8). For the three samples studied here p is equal to 0.02, 0.12 and 0.23 for, respectively, samples Y1, Y2 and Y3. These values have been obtained by using in equations (8) and (9), $C_1 = 0$ and $C_2 = 0.5 \ \mu\Omega \ K^{-1}$.

In analogy with equation (8) for $\rho(T)$, we may introduce an empirical relationship between the measured thermopower in *single-phase* granular samples, $S(T)$, with the intrinsic thermopower in the ab plane, S_{ab}, in an ideal single crystal of the same composition. For that, we may assume first that in measuring S, an intensive magnitude, the random distribution of the ab planes and c directions of the grains, crystallites and untwinned domains in a polycrystalline sample is equivalent to a sample having ab and c paths in parallel [34]. So, by applying equation (2), the equivalent thermopower S^e is easily found to be

$$S^e = (S_{ab}\sigma_{ab} + S_c\sigma_c)/(\sigma_{ab} + \sigma_c) \simeq S_{ab} \tag{10}$$

where we have assumed $\sigma_{ab} \gg \sigma_c$ [33], whereas S_{ab} and S_c are of the same order of magnitude in $Y_1Ba_2Cu_3O_{7-\delta}$ samples [20–23]. Now, the differences between S and S^e are due to the presence in the real granular sample of intergrains and interfaces, having some effective thermal resistivity and thermopower. So, we may suppose that only a fraction, $p^s\Delta T$, of the temperature difference (ΔT) used to measure S arises through the intragrains, the other fraction, $(1 - p^s)\Delta T$, being associated with the intergrains and interfaces. Therefore, $S(T)$ may be crudely related to $S_{ab}(T)$ by

$$S(T) = p^s S_{ab}(T) + S_{ct}(T) \tag{11}$$

where p^s ($0 < p^s \leqslant 1$) is the coefficient that takes into account the relative gradient temperature distribution between intragrains and intergrains, $S_{ct} \equiv (1 - p^s)S_{ct}^e$ will be the contribution to $S(T)$ associated with the sample interdomains (grains, crystallites, untwinned regions) and S_{ct}^e is the 'effective' thermopower of these sample interfaces.

Note that above but near the superconducting transition of the intragrains, the possible temperature dependence not only of p^s but also of S_{ct} will be very weak when compared with that of $S_{ab}(T)$. So equation (11) may easily explain various important qualitative aspects of $S(T)$ as was the case of equation (8) for the measured resistivity in granular samples [4–7]. For instance, in the absence of an applied magnetic field, we may define the critical transition temperature of the intragrains, T_{CI}^S, through $S(T)$ as

$$(d^2 S/dT^2)_{T_{CI}^S} = 0. \tag{12}$$

In excellent agreement with our experimental findings, equation (12) predicts that T_{CI}^S will be almost the same for all the different samples with the same nominal composition. In addition, T_{CI}^S and T_{CI} are also reasonably similar, their differences for the three samples studied here being well inside $\Delta T_{CI} \simeq 0.3$ K. So, the mean-field reduced critical temperatures ϵ may be approximated as

$$\epsilon = \ln(T/T_{CI}) \tag{13}$$

for both $S(T)$ and $\sigma(T)$. Note, finally, that in the background region, far from the transition, S_{cl} is much more sensitive than ρ_{cl} to local inhomogeneities and impurities and, therefore, has a more complicated temperature dependence. So, $S_{ab}(T)$ cannot be extracted from equation (11) by following a procedure similar to that which we have used for $\rho(T)$, which assumes ρ_{cl} and p to be temperature-independent.

4. Data analysis and comparison with theoretical approaches

We are now able to extract and to compare the corresponding *excesses* with one another and with the existing theories, which may be defined as

$$\Delta S(\epsilon) \equiv S_{\mathrm{B}}(\epsilon) - S(\epsilon) \tag{14}$$

$$\Delta \sigma(\epsilon) \equiv \sigma(\epsilon) - \sigma_{\mathrm{B}}(\epsilon) \tag{15}$$

$$\Delta L(T) \equiv L(T) - L_{\mathrm{B}}(T) = S(T)\sigma(T) - S_{\mathrm{B}}(T)\sigma_{\mathrm{B}}(T) \tag{16}$$

for, respectively, $S(\epsilon)$, $\sigma(\epsilon)$ and the thermopower coefficient $L(T)$, defined by equation (1). In these expressions, the quantities denoted with the subscript B are the corresponding backgrounds, i.e. the magnitudes not affected by the OPF effects. They are obtained by extrapolating through the transition the T behaviour of the corresponding quantities in the normal region, as indicated before. Note that $\Delta L(\epsilon)$ may be directly related to $\Delta S(\epsilon)$ and $\Delta \sigma(\epsilon)$ by just using the above definitions, as

$$\Delta L(\epsilon)/L_{\mathrm{B}}(\epsilon) = \Delta \sigma(\epsilon)/\sigma_{\mathrm{B}}(\epsilon) - (\sigma(\epsilon)/\sigma_{\mathrm{B}}(\epsilon))\Delta S(\epsilon)/S_{\mathrm{B}}(\epsilon). \tag{17}$$

Let us also stress that these expressions for the three excesses are very general, and they do not depend on any particular model for the OPF effects on the three magnitudes involved, $S(\epsilon)$, $\sigma(\epsilon)$ and $L(\epsilon)$. Equations (14) to (17) concern, as noted already, the *measured* magnitudes. However, the same procedure may be directly applied to the magnitudes for the ab plane of an ideal single crystal, and they are going to be denoted by the subscript ab. For instance, in the case of the excess of the thermopower coefficient, we have

$$\Delta L_{ab}(\epsilon) \equiv L_{ab}(\epsilon) - L_{abB}(\epsilon) = S_{abB}\Delta \sigma_{ab}(\epsilon) - \sigma_{ab}(\epsilon)\Delta S_{ab}(\epsilon) \tag{18}$$

which may be seen as the limit of equation (17) to the ideal single crystal with the same nominal composition as the measured polycrystalline sample. Note also that from equations (11) and (14), we may directly obtain

$$\Delta S(\epsilon) = p^{s}\Delta S_{ab}(\epsilon) \tag{19}$$

relating the measured thermopower excess with the intrinsic one in the ab plane. This equation indicates that the ϵ dependence of ΔS will be the same for all the *single-phase* samples having the same composition, independently of their long length scale *structural* inhomogeneities. This conclusion is verified by our samples within
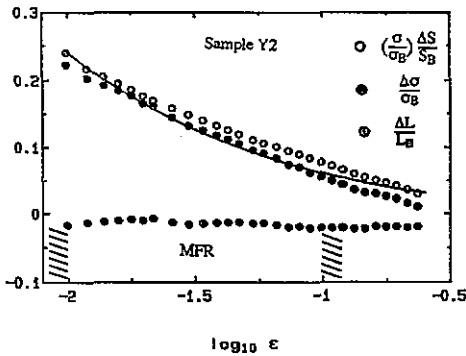
Figure 4. Normalized excesses of $S(T)$ (open circles), $\sigma(T)$ (full circles) and $L(T)$ (dotted circles) versus the logarithm of the reduced temperature for sample Y2. The full curve is the best fit of the Lawrence–Doniach approach of the normalized paraconductivity in the indicated mean-field-like region (MFR).
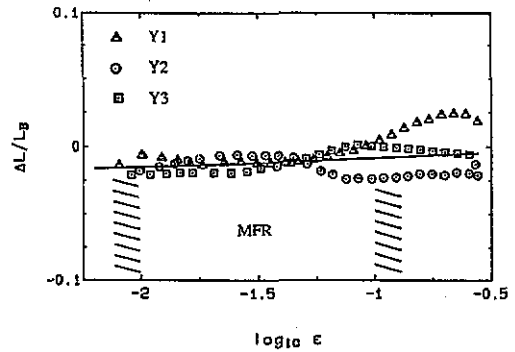
Figure 5. Normalized excess of the thermoelectric coefficient versus reduced temperature for three different YBCO samples. The full curve represents the best fit of Maki's approach for layered superconductors.

10%. From equation (19) we may then conclude that the ϵ dependence of $\Delta S/S_B$ will be very close to the intrinsic one.

As an example, in figure 4 we plot the two contributions to $\Delta L(\epsilon)/L_B(\epsilon)$ in equation (17), $\Delta\sigma(\epsilon)/\sigma_B(\epsilon)$ and $(\sigma/\sigma_B)\Delta S(\epsilon)/S_B(\epsilon)$, as a function of $\log_{10}\epsilon$ for one of the samples (Y2). These experimental results clearly show that $\Delta\sigma(\epsilon)/\sigma_B(\epsilon)$ and $(\sigma/\sigma_B)\Delta S(\epsilon)/S_B(\epsilon)$ have very similar *amplitude* and *reduced temperature behaviour*, over all the ϵ range examined. Therefore, as shown also in this figure, $\Delta L(\epsilon)$, the corresponding experimental thermopower coefficient excess, is almost reduced-temperature-independent, and it has a very small negative amplitude, which may be approximated as zero to within the experimental uncertainties. Note that our previous results [4–7] for $\Delta\sigma(\epsilon)$ and $\Delta\chi(\epsilon)$ clearly suggest that the ϵ range studied here spans all the MFR. Similar results to those shown in figure 4 are also obtained for the other two samples studied here, which have distinct structural inhomogeneities at large length scales, as shown for $\Delta L(\epsilon)/L_B(\epsilon)$ in figure 5. So, we may conclude that, to within the experimental uncertainties of $\Delta L/L_B \gtrsim 2\%$, $\Delta L_{ab}(\epsilon) \simeq 0$ over the MFR. Our present results fully confirm at a quantitative level our previous experimental findings for YBCO [12, 13] or Bi-based samples [19], and provide strong evidence that the critical behaviour of $S(\epsilon)$ in HTSC is essentially driven by that of $\sigma(\epsilon)$. The full line in figure 4 has been obtained by using for $\Delta\sigma(\epsilon)$ the expression proposed by the Lawrence–Doniach (LD) theory [35]. As expected from previous paraconductivity [4–7] comparisons, the agreement of the experimental $\Delta\sigma(\epsilon)/\sigma_B(\epsilon)$ with the theoretical ϵ behaviour is excellent over all the MFR. The fitting parameters of the LD approach confirm the 3D nature of OPF in the MFR of $Y_1Ba_2Cu_3O_{7-\delta}$ compounds, as explained in [4, 5] (see also later). Finally, it is interesting to note here that, by combining the result $\Delta L \simeq 0$ with equations (8), (11) and (17), we may obtain useful relationships in the MFR between the measured $L(T)$ and the corresponding intrinsic thermopower coefficient: $L(T) = p^s p L_{ab}(T)$. It is also easy to obtain $S_{ct}(T) = \rho_\alpha L(T)/p$.

We are now able to compare our data for $\Delta L(\epsilon)$ with the available theory

[2, 27, 36]. In particular, to our knowledge it will be the first time that the theoretical results of Maki [27] for $\Delta L(\epsilon)$ in *layered* superconductors have been compared with the experiments in HTSC. Unfortunately, all the existing theoretical approaches for $\Delta L(\epsilon)$ in the MFR mainly focus on its reduced temperature behaviour, and a tractable estimate of its amplitude has not been published yet, although it is recognized that it must probably be very small [2, 27], in full agreement with our experimental findings presented here and in previous papers [12, 13]. As a consequence, it is clear that nearly any functional form for $\Delta L(\epsilon)$ can fit the data if a small enough amplitude is used. In spite of these difficulties, we compare in figure 5 our experimental data for $\Delta L(\epsilon)$ with the theoretical expression proposed by Maki for s-wave layered superconductors in the clean limit [27]

$$\Delta L(\epsilon) = A_{\rm L} \ln \left\{ 4/\epsilon[1 + (1 + 2\alpha)^{1/2}]^2 \right\} \tag{20}$$

where

$$A_{\rm L} \equiv [(2\pi T)^2/7\zeta(3)]\lambda e\tau/d_{\rm e} \tag{21}$$

$$\alpha \equiv 2[\xi_{\rm c}(0)/d_{\rm e}]^2/\epsilon \tag{22}$$

$$\lambda \equiv (2\pi T/gN_0)\partial \ln N_0/\partial\mu. \tag{23}$$

In the above expressions, g is the electron–phonon coupling constant, N_0 is the electron density of states, μ is the chemical potential, τ is the scattering lifetime, $\zeta(3) = 1.202$, $\xi_{\rm c}(0)$ is the superconducting correlation length amplitude (for $T = 0$) in the c direction, and $d_{\rm e}$ is the effective interlayer distance, which takes into account that in YBCO compounds there exist inequivalent conducting layers at different distances and with a different effective Josephson coupling. A somewhat disturbing feature of equation (20) is that its limits for $\alpha \ll 1$ or $\alpha \gg 1$ do not agree with previous calculations for films (2D) or bulk (3D) materials [2, 36]. Although the latter cases were calculated in the dirty limit, the discrepancies remain even for the ϵ dependence. In any case, the data points in figure 5 correspond to our experimental data of $\Delta L(\epsilon)$ obtained for each of the three YBCO samples studied here, whereas the full line has been obtained from equation (20), with $d_{\rm e} = 11.7$ Å and $\xi_{\rm c}(0) = 2$ Å, and $A_{\rm L}$ as a free parameter. These values, which agree with those currently proposed in the literature [37], are determined by applying the Lawrence–Doniach approach to our previous measurements of $\Delta\sigma(\epsilon)$ and of $\Delta\chi(\epsilon)$ in the MFR [4–7] by assuming that the number of effective superconducting planes ab per unit cell length is $N = 1$ and $\xi_{ab}(0) = 14$ Å. The same values are obtained from $\Delta\chi(\epsilon)$ by using $N = 2$ and $\xi_{ab}(0) = 10$ Å. In this last case the measured $\Delta\sigma_{ab}(\epsilon)$ amplitude may simultaneously be explained by the presence of only direct OPF effects. Note that in the MFR, $\xi(\epsilon) \gtrsim d_{\rm e}$, so the OPF in that region will be essentially 3D, in agreement with our previous results for the paraconductivity and the paradiamagnetism [4–7]. Concerning $\Delta L(\epsilon)$, and as noted above, the reasonable agreement between the theory and the experimental data found in figure 5 does not allow us to conclude anything about the adequacy of the ϵ dependence of equation (20). In fact, this comparison allows us only to propose an upper limit to $A_{\rm L}$ in the MFR, which is of the order of 40 μA cm^{-1} K^{-1}. This is, indeed, a very small amplitude when compared with that of $\sigma\Delta S(\epsilon)$ in the same ϵ range (see figure 4), in agreement with the qualitative Maki suggestions [2, 27]. A more detailed calculation of $A_{\rm L}$ in terms of more directly experimentally accessible parameters will allow a more quantitative comparison.

5. Conclusions

We have reported detailed data of the thermopower coefficient $L(T)$ above the superconducting transition of three single-phase (to 4%) polycrystalline $Y_1Ba_2Cu_3O_{7-\delta}$ samples (with $\delta \lesssim 0.10$). These data strongly suggest, for the first time to a quantitative level in any superconducting transition, that $L(T)$ is not affected by the presence of important thermodynamic fluctuations of the superconducting order parameter amplitude (OPF). In other words, all the critical effects observed in the thermoelectric power $S(T)$ above the superconducting transition will be due to those of the electrical conductivity. These findings seem to be confirmed, at least at a qualitative level, by recent theoretical calculations of the excess of the thermopower coefficient in the mean-field-like region in layered superconductors [27]. Our results fully confirm that the order parameter fluctuations in the mean-field-like region of $Y_1Ba_2Cu_3O_{7-\delta}$ compounds are essentially three-dimensional (3D). Also, to within our experimental resolutions, no fractal behaviour is observed in our granular single-phase samples, i.e. the reduced temperature behaviour of the thermopower excess $\Delta S(\epsilon)$ is the same for all the different single-phase samples studied here. Although new measurements in good single-crystal samples will be very useful to confirm these results, we believe that the essential aspects of the OPF influence on the thermoelectric power in $Y_1Ba_2Cu_3O_{7-\delta}$ samples are those presented in this work.

References

[1] Ginzburg V L 1989 *Physica* C **162-4** 277; 1989 *J. Supercond.* **2** 323; 1991 *Supercond. Sci. Technol.* **4** S1 and references therein
[2] Maki K 1974 *J. Low Temp. Phys.* **14** 419
[3] Skocpol W J and Tinkham M 1975 *Rep. Prog. Phys.* **38** 1049
[4] Veira J A and Vidal F 1989 *Physica* C **159** 468; earlier references on the OPF effects on the electrical conductivity are given here
[5] Veira J A and Vidal F 1990 *Phys. Rev.* B **42** 8748
[6] Vidal F , Torrón C, Veira J A, Miguélez F and Maza J 1991 *J. Phys.: Condens. Matter* **3** 5219, 9257; earlier references on the OPF effects on the magnetic susceptibility are given here
[7] Torrón C, Cabeza O, Veira J A, Maza J and Vidal F 1992 *J. Phys.: Condens. Matter* **4** 4273
[8] Trodahl H J and Mawdsley A 1987 *Phys. Rev.* B **36** 8881
[9] Laurent Ch, Patapis S K, Laguesse M, Vanderschueren H W, Rulmont A, Tarte P and Ausloos M 1988 *Solid State Commun.* **66** 445
[10] Clippe P, Laurent Ch, Patapis S K and Ausloos M 1990 *Phys. Rev.* B **42** 8611
[11] Dey T K, Ghatak S K, Srinivasan S, Bhattacharya D and Chopra K L 1989 *Solid State Commun.* **72** 525

       Dey T K, Radha K, Barik H K, Bhattacharya D and Chopra K L 1990 *Solid State Commun.* **74**
       1315
[12]   Cabeza O, Yadava Y P, Maza J, Torrón C and Vidal F 1991 *Physica* C **185–9** 1897
[13]   Cabeza O, Yadava Y P, Veira J A, Maza J, Vidal F, Casais M T, Cascales C and Rasines I 1992
       Properties and Applications of Perovskite-Type Oxides ed L G Tejuca and J L Fierro (New York:
       Dekker) in press
[14]   Bhatnagar A K, Pan R, Naugle D G, Gilbert G R and Pandey R K 1990 *Phys. Rev.* B **41** 4002
       Cohn J L, Skelton E F, Wolf S A and Liu J L 1992 *Phys. Rev.* B **45** 13 140
[15]   Uher C and Kaiser A B 1987 *Phys. Rev.* B **36** 5680
[16]   Howson M A, Salamon M B, Friedmann T A, Inderhees S E, Rice J P, Ginsberg D M and Ghiron
       K M 1989 *J. Phys.: Condens. Matter* **1** 465
       Howson M A, Salamon M B, Friedmann T A, Rice J P and Ginsberg D 1990 *Phys. Rev.* B **41** 300
       Lowe A J, Regan S and Howson M A 1991 *Phys. Rev.* B **44** 9757
[17]   Yan S S, Chen T, Zhang H, Peng J, Shen Z, Wei C, Wen Q, Wu K and Tong L 1988 *Mod. Phys.*
       Lett. B **2** 1005
[18]   Laurent Ch, Patapis S K, Green S M, Luo H L, Politis C, Durczewski K and Ausloos M 1989 *Mod.*
       Phys. Lett. B **3** 241
[19]   Lopez A J, Maza J, Yadava Y P, Vidal F, García-Alvarado F, Morán E and Señaris-Rodríguez
       M A 1991 *Supercond. Sci. Technol.* **4** S292
[20]   Wang Z Z and Ong N P 1988 *Phys. Rev.* B **38** 7160
[21]   Sera M, Shamoto S and Sato M 1988 *Solid State Commun.* **68** 649
[22]   Li L, Bei-Hai M, Shu-Yuan L, Hong-Min D and Dian-Lin Z 1988 *Europhys. Lett.* **7** 555
[23]   Kaiser A B and Mountjoy G 1991 *Phys. Rev.* B **43** 6266
[24]   Yu R C, Naughton M J, Yan X, Chaikin P M, Holtzberg F, Greene R L, Stuart J and Davies P
       1988 *Phys. Rev.* B **37** 7963
[25]   Lin Shu-Yuan, Lu Li, Duan Hong-Min, Ma Bei-Hai and Zhang Din-Lin 1989 *Int. J. Mod. Phys.* B
       3 409
[26]   Cohn J L, Wolf S A, Selvanikov V and Salama K 1991 *Phys. Rev. Lett.* **66** 1098 and references
       therein
[27]   Maki K 1991 *Phys. Rev.* B **43** 1252, 13 685 (erratum)
[28]   Amador J, Cascales C and Rasines I 1988 *High-Temperature Superconductors* ed M B Brodsky, R C
       Dynes, K Kitazawa and H L Tuller (Pittsburgh, PA: Materials Research Society) p 249
[29]   Callen H B 1966 *Thermodynamics* (New York: Wiley) ch 17
[30]   Blatt F J, Schroeder P A, Foiles C L and Greig D 1976 *Thermoelectric Power of Metals* (New York:
       Plenum)
[31]   Srinivasan R, Sandaranarayan V, Raju N P, Natarajan S, Varadaju U V and Subba Rao G V 1987
       Pramana–J. Phys. **29** L225
       Mukherjie C D, Ranganathan R, Raychandhuri A K and Chatterejee N 1989 *Phys. Status Solidi* B
       154 K55
       Radharkrishnan V, Subramanian C K, Sankaranarayanan V, Subba Rao G V and Srinivasan R 1989
       Phys. Rev. B **40** 6850
[32]   Maza J and Vidal F 1991 *Phys. Rev.* B **43** 10 560
[33]   Hagen S J, Jing T W, Wang Z Z, Horvath J R and Ong N P 1988 *Phys. Rev.* B **37** 7928
       Friedmann T A, Rice J P, Giapintzakis J and Ginsberg D M 1989 *Phys. Rev.* B **39** 4258
       Hikita M and Suzuki M 1990 *Phys. Rev.* B **41** 834
       Friedmann T A, Ravin M W, Giapintzakis J, Rice J P and Ginsberg D M 1990 *Phys. Rev.* B **42**
       6217
       Winzer K and Kumm G 1991 *Z. Phys.* B **82** 317
       Rice J P, Giapintzakis P M, Ginsberg P M and Mochel J M 1991 *Phys. Rev.* B **44** 10 158
[34]   Ausloos M, Durczewski K, Patapis S K, Laurent Ch and Vanderschueren H W 1988 *Solid State*
       Commun. **65** 365
[35]   Lawrence W E and Doniach S 1971 *Proc. 12th Int. Conf. on Low-Temperature Physics (Kyoto, Japan,*
       1970) ed E Kanda (Tokyo: Keigatu) p 361
       Klemm R A 1990 *Phys. Rev.* B **41** 2073
       Yip S 1990 *J. Low Temp. Phys.* **81** 129
[36]   Ullah S and Dorsey A T 1991 *Phys. Rev.* B **44** 262
[37]   Batlogg B 1992 *Physics of High-Temperature Superconductors* ed S Maekawa and M Sato (Berlin:
       Springer) p 219